NATIONAL ADVISORY COMMITTEE FOR AERONAUTICS

TECHNICAL NOTE

No. 1690

THEORETICAL AND EXPERIMENTAL WING-TIP ACCELERATIONS OF A SMALL FLYING BOAT DURING LANDING IMPACTS

By Daniel Savitsky

Langley Aeronautical Laboratory
Langley Field, Va.

Washington

September 1948

NATIONAL ADVISORY COMMITTEE FOR AERONAUTICS

TECHNICAL NOTE NO. 1690

THEORETICAL AND EXPERIMENTAL WING-TIP ACCELERATIONS OF A SMALL FLYING BOAT DURING LANDING IMPACTS

By Daniel Savitsky

SUMMARY

A simplified analytical method for predicting the time history of the accelerations along the wing of an airplane during landing impact is presented and compared with wing-tip-acceleration data obtained from full-scale landing tests of a small seaplane. The structural properties of the seaplane were such that only the fundamental wing bending mode of vibration had an important effect on the wing-tip accelerations and the over-all structural properties had little effect on the hydrodynamic impact force. For these conditions, the theoretical and experimental time histories of wing-tip acceleration show very good agreement.

A sine curve is used as an approximation for the force-time variation of the measured impact force and agrees fairly closely with the experimental impact-force time histories up to and somewhat beyond the time of maximum impact load.

Where the most severe impacts of the tested seaplane occurred subsequent to the initial impact of a particular landing, the seaplane bounce that preceded this severe impact was usually sufficiently high and of long enough duration to stop the wing vibrations excited by the prior impact.

INTRODUCTION

The construction of large flexible airplanes has increased the importance of evaluating the effects of airframe elasticity in producing critical design loads in the structure during landing impact. In order to enable the designer to calculate these dynamic inertia loads without having to employ the lengthy and tedious calculations required for an exact solution of the problem, various theoretical methods for a relatively simple and quick solution of the structural elasticity problems have been developed. Several of these solutions are described in references 1 and 2. Although each of these simplified methods is based on advanced vibration theory, the resultant final solutions presented in each have certain limitations so that they are not generally applicable to all phases of the structural response problem.

Measurements were made of the resulting wing-tip accelerations during impact for a series of full-scale landing tests of a small seaplane. A comparison of these experimental wing-tip accelerations with calculated values obtained by application of a simplified theoretical solution was desired. Direct application of the existing theoretical methods (references 1 and 2) for the analytical evaluation of the wing-tip accelerations of the test seaplane was not feasible, however, for several reasons. Two of the reasons are: First, although reference 1 proposes detailed methods for evaluating the stress distribution throughout an airframe subjected to landing impact, this reference does not treat specifically the problem of determining the acceleration distribution throughout the structure, which may be critical in the local structural design. Second, although reference 2 presents a solution for the evaluation of accelerations that considers the effect of structural elasticity in altering the impact force, the scale of the plots of the generalized results presented in this reference is such that inaccurate answers are obtained when there is only a small difference between the acceleration of the nodal point of a wing bending mode and the acceleration of the hull, as was the case for the tested seaplane. Thus, since the final results of the existing solutions were not directly applicable to the prediction of accelerations for the tested seaplane, the basic theories of vibration as discussed in references 1 and 2 were considered in this paper, and a simplified method based on these theories was developed for the evaluation of the time history of the acceleration distribution throughout an airplane structure subjected to landing impact when the impact-force time history can be defined by a simple mathematical curve.

This paper presents the development of the simplified method and illustrates its application to the determination of the wing-tip accelerations during landing impacts of the tested seaplane. A comparison of the computed and the measured wing-tip-acceleration time histories is presented for the severe landing impacts of the seaplane, and a comparison of the computed and the measured maximum wing-tip accelerations is given for the light impacts. The calculations concerned with the determination of the transient-oscillatory-acceleration response of an airframe to sine-curve forcing functions are given in an appendix.

SYMBOLS

t_n time required for one-fourth of a cycle of natural vibration, seconds

t_i time between initial water contact and maximum hydrodynamic force, seconds

t	time elapsed after initial water contact, seconds
C_t	time coefficient $\left(t\left(\frac{0.0525}{t_n}\right)\right)$
w	increment of weight, pounds
n_i	maximum impact acceleration normal to water surface in multiples of the acceleration due to gravity
m	increment of mass, pound-second^2 per foot (w/g)
M	total mass of seaplane, pound-second^2 per foot
W	total weight of seaplane, pounds
g	acceleration due to gravity, feet per second per second
ω_n	natural circular frequency of wing bending mode, radians per second $\left(\left(\frac{1}{4t_n}\right)2\pi\right)$
ω_i	equivalent circular frequency of applied force, radians per second $(\pi/2t_i)$
$P(t)$	time variation of applied impact force
P_{max}	maximum value of applied impact force, pounds
ϕ	proportionality factor defining wing deflection curve for fundamental bending mode in terms of unit deflection of wing tip
ϕ'	proportionality factor defining wing deflection curve for secondary bending mode
k	spring constant of single-mass oscillator, pounds per foot
k_e	effective spring constant at any wing station, pounds per foot
y_o	translational displacement of wing nodal point, feet
y_t	wing-tip displacement with respect to nodal point, feet
y_r	resultant displacement of any point on wing, feet
$\bar{M}$	effective mass $(\Sigma m\phi^2)$
x	distance along wing outboard from center line, feet

Subscripts

x	any wing station
p	point of application of impact force

METHOD OF ANALYSIS

When an airplane lands, the resultant displacement y_r of any point on the wing may be considered to be composed of two parts, as is shown in the simplified representation in figure 1. One component of motion is that resulting from the translation of the airplane as a rigid body (fig. 1(b)). The other is the motion of that point resulting from the transient oscillatory motion of each of the natural modes of vibration of the wing structure excited by the impact force (fig. 1(c)). Thus:

$$y_r = y_o + \phi y_t \tag{1}$$

The term y_o in equation (1) is the rigid-body displacement of the airplane, which is also the displacement of the nodal points of any wing mode. The term ϕy_t represents the displacement relative to the nodal point of any point on the structure when the wing is deflected in a normal mode shape, where ϕ is the space function defining that normal mode shape. For convenience, in this paper ϕ is defined in terms of a unit deflection of the extreme wing tip relative to the nodal point, although it could be defined in terms of the deflection of any other point on the deflected wing. The term y_t is the deflection of the extreme wing tip in a normal mode. A separate value of ϕy_t is included in equation (1) for each of the wing modes concerned; however, for simplicity, the effect of only one mode will be discussed. The evaluation of the effects of other modes follows an identical procedure and the deflections associated with each mode are superposed to obtain resultant deflections.

From equation (1) the resultant acceleration of any point on the wing is readily seen to be:

$$\ddot{y}_r = \ddot{y}_o + \phi \ddot{y}_t \tag{2}$$

The translational acceleration $\ddot{y}_o$ is obtained from Newton's second law of motion and is equal to

$$\ddot{y}_o = P(t)/M \tag{3}$$

The transient oscillatory component of acceleration $\ddot{y}_t$ is obtained from the Lagrangian equation defining the motion of the wing structure when the wing oscillates in a natural mode. A derivation of this equation is included in reference 1. This equation of motion is written as:

$$\bar{M}\ddot{y}_t + \bar{M}\omega_n^2 y_t = P(t)\phi_p \tag{4}$$

where $\bar{M}$ is equal to $\Sigma m\phi^2$ and ϕ_p is the deflection of the point of application of the impact force relative to the nodal point for a unit wing-tip deflection.

Rearranging equation (4) and substituting $\Sigma m\phi^2$ for $\bar{M}$ results in the equation:

$$\frac{\Sigma m\phi^2}{\phi_p}\ddot{y}_t + \omega_n^2 \frac{\Sigma m\phi^2}{\phi_p} y_t = P(t) \tag{5}$$

Equation (5), the solution of which yields the transient oscillatory component of acceleration at the extreme wing tip, is the differential equation of motion of an undamped, single-mass, linear oscillator. Thus, the evaluation of the oscillatory component of acceleration for the wing tip has been reduced to the relatively simple solution of the equation of motion of a single-mass oscillator, the natural frequency of which is equal to the frequency ω_n of the mode being considered, and the spring constant of which is equal to the term $\omega_n^2 \frac{\Sigma m\phi^2}{\phi_p}$ appearing in equation (5). This spring-constant term $\omega_n^2 \frac{\Sigma m\phi^2}{\phi_p}$ for the extreme wing tip will be shown to be physically equal to the ratio of the force causing the wing beam to deflect in one of its natural modes to the resultant wing-tip deflection relative to the nodal point. Equating the work done by the external force in deflecting the wing beam in a natural mode to the internal strain energy of the wing expressed in terms of the kinetic energy in the wing when it

is released from its position of maximum deflection corresponding to P_{max} and passes through a position of zero deflection, results in the expression

$$\frac{P_{max}\phi_p y_t}{2} = \frac{\omega_n^2}{2}\Sigma m\left(\phi y_t\right)^2 \tag{6}$$

Equation (6) can be rearranged to result in the value of the effective spring constant at the extreme wing tip $k_{e_{tip}}$ as defined previously:

$$k_{e_{tip}} = \frac{P_{max}}{y_t} = \omega_n^2 \frac{\Sigma m\phi^2}{\phi_p} \tag{7}$$

The last term in equation (7) is equal to the multiplying factor of y_t in equation (5). An equivalent constant k_{e_x} for any other point x on the wing can readily be found from a knowledge of the proportionality factor ϕ_x at that station and $k_{e_{tip}}$. Thus:

$$k_{e_x} = \frac{k_{e_{tip}}}{\phi_x} \tag{8}$$

Since the vibratory characteristics of any point on the wing have been defined in terms of k_e and ω_n, the vibratory characteristics of the equivalent linear single-mass oscillator for that point are also known. The mass of this equivalent oscillator is a fictitious or "effective" mass equal to k_e/ω_n^2. Thus, substituting the terms just defined in the differential equation of motion of a single-mass oscillator results in the equation of motion for the equivalent single-mass oscillator at any point x along the wing

$$\frac{k_{e_x}}{\omega_n^2}\ddot{y}_x + k_{e_x}y_x = P(t) \tag{9}$$

Solving the equations of motion of the equivalent oscillator for $\ddot{y}_x$, the transient oscillatory acceleration at any wing station x, and adding this component of acceleration to the translational acceleration as defined by equation (3) gives the total acceleration at any point x on the wing. Although the preceding discussion was limited to the evaluation of the effects of but one mode, higher modes are treated in a similar

manner. That is, an equivalent linear oscillator is found for each normal mode and the oscillatory accelerations associated with each oscillator are superposed.

The forcing function $P(t)$ in equations (3) and (5) is the time history of the external impact force applied to the airplane during landing. In the case of a seaplane subjected to landing impact, this forcing function is the time history of the hydrodynamic impact force, which, when expressed in terms of gross weight of seaplane, is equal to the translational or nodal acceleration. If this forcing function can be expressed by a simple mathematical curve, the solution of the equation of motion of the single-mass oscillator for the oscillatory acceleration can be simply obtained. The calculations included in the appendix illustrate the derivation of the transient-oscillatory-acceleration response of a single-mass oscillator to a sine-curve variation of the forcing function. The sine curve is used in this derivation since, as is shown in a subsequent section of this paper, it could be used as a close approximation to the time history of experimentally obtained hydrodynamic impact forces. The response to other simplified mathematical curves can be treated in a similar fashion.

APPARATUS AND TEST PROCEDURE

Seaplane

The seaplane used in the tests was a twin-engine amphibian having an angle of dead rise of 20° at the step. A three-view sketch of the seaplane together with pertinent dimensions is given in figure 2. The wing was attached to the hull by means of support struts and tie rods mounted on the outboard side of each of the engine mounts. The vertical pylon between the center of the wing and the hull is a non-structural fairing and does not transmit any of the wing inertia loads to the hull. The gross weight of the seaplane during the landing tests was approximately 19,000 pounds. A detailed tabulation of the weight distribution along the seaplane wing, as obtained from data supplied by the manufacturer, is given in table I.

The natural frequencies and mode shapes of the seaplane were obtained from ground vibration tests. The amphibian was supported on its landing gear and the wing was vibrated by means of an electromagnetic vibrator connected to the main spar near the left wing tip (fig. 3). In order to investigate the effect that the method of seaplane support has on the wing frequencies and mode shapes, several vibration surveys were conducted over a range of tire pressures and with the oleo strut locked and unlocked. All methods of support resulted in substantially identical wing frequencies and mode shapes. Figure 4 presents a sketch of the first and second mode shapes. A tabulation of the mode-shape factors

for wing deflection relative to the nodal points based on unit tip deflection is given in table I.

Instrumentation

Time histories of the impact accelerations normal to the keel were measured by three induction-type accelerometers which were installed as follows: one at the seaplane center of gravity, another just inboard of the right engine, and a third near the right wing tip (fig. 2). In the following discussion, the accelerometer at the center of gravity will be referred to as the hull accelerometer and the accelerometer near the wing tip will be designated the wing-tip accelerometer. The accelerometers had an undamped natural frequency of 60 cycles per second, were oil-damped to approximately 0.6 critical, had an accuracy of approximately $\pm$0.2g, and were simultaneously recorded on a multichannel oscillograph.

Test Procedure

The landing-impact tests were made in smooth water. Since the primary purpose of these tests was to determine the hydrodynamic impact loads on the hull, landings were made over a range of trims and flight-path angles. For the purpose of this paper, however, only those impacts were considered wherein the forebody made contact with the water first and the wing was substantially free of extraneous vibrations just prior to impact. In the case of initial afterbody contacts, the seaplane usually rotated forward to result in superposed forebody impact and thus made impractical an exact mathematical definition of the primary hydrodynamic forcing function.

RESULTS AND DISCUSSION

Experimental

A tabulation of the values of maximum hull acceleration, time to maximum hull acceleration (impact period), and maximum wing-tip acceleration recorded during the various test runs is presented in table II. The impact accelerations measured in the vicinity of the right engine are not presented herein since this accelerometer had a considerable amount of high-frequency hash superposed and so made a reliable estimate of the record deflection very difficult. The wing-tip accelerations were always larger than the hull accelerations by an amount that varied approximately inversely as the impact period. (See table II.)

A plot of the recorded time histories of the hull and corresponding wing-tip accelerations is presented in figure 5 for the three most severe impacts. (Tests 2, 3, and 7.) A considerable amount of irregularity is seen to exist in the record traces of the hull accelerations. As an attempt to define the time history of the hull accelerations by a simple mathematical expression, a sine curve was plotted over the record trace with the peak acceleration as maximum ordinate and the impact period as the time for one-quarter cycle. Figure 5 presents a comparison between the assumed sine curves faired through all three record traces and the measured impact force and shows that the sine curve can be used as a satisfactory approximation up to and somewhat beyond the time of maximum hull acceleration. Although the results are not included in this paper, a comparison was also made between the sine curve and measured hull-acceleration time histories for the other test runs listed in table II. This comparison showed that the sine curve could be used as a close approximation for the other runs also. Although the sine-curve approximation can be used for the impact conditions encountered with the test seaplane, for airplanes wherein the structural elasticity has an appreciable effect on altering the impact force or in landings wherein the flight path is very shallow or steep a sine-curve approximation may not be suitable. Theoretical time histories of the hydrodynamic forcing function for a range of landing conditions and airplane elasticities are given in references 2 and 3.

The wing-tip-acceleration time histories are plotted directly below the corresponding hull accelerations and indicate that the wing tip reaches a peak acceleration at some time subsequent to peak impact load. During the first part of the impact, the tip acceleration is slightly positive as a result of the superposition of the transient oscillatory acceleration upon the impact translational acceleration. In comparison with tests 2 and 3, the record trace of tip acceleration for test 7 is somewhat irregular since at the time of this impact some extraneous wing vibrations were present in the wing structure prior to initial impact. Nevertheless, the general pattern of that time history is readily distinguishable.

As shown in table II some of the wing-tip-acceleration data were obtained from the second, third, and fourth impacts of any particular landing. For most of these subsequent impacts the wing vibrations excited by the preceding impact were sufficiently diminished between impacts by the structural and aerodynamic damping to consider the oscillations of the structure set up by one impact to be almost completely independent of the oscillations set up by any preceding impact. If, during the seaplane rebound from the water surface that is usually associated with a hydrodynamic impact, the seaplane was not completely airborne for a sufficient length of time, the wing oscillations were not completely damped out. For most of the severe smooth-water impacts, however, the rebound that preceded the impact was high enough and of long enough duration to allow almost complete damping out of the wing vibrations. The data from those light impacts in which the

vibrations were not materially reduced during the preceding rebound are not presented herein.

Calculated

Application of the analytical procedures described in the section entitled "Method of Analysis" is illustrated in the following paragraphs for the determination of the translational component, the transient oscillatory component, and the resultant of the wing-tip accelerations of the tested seaplane during landing impact. Calculated and experimental wing-tip accelerations referred to in this paper are for the wing station at which the outboard accelerometer is located (450 in. from center line) unless otherwise specified. Time histories of the resultant wing-tip accelerations were calculated for the three most severe impacts (tests 2, 3, and 7) but only the maximum resultant accelerations were calculated for the remaining impacts. These calculated values are compared with the experimental data obtained from full-scale landings of the test seaplane.

Translational component of acceleration.- The time history of the translational acceleration of the seaplane is equal to the time history of the hydrodynamic impact force expressed in multiples of the gross weight of the seaplane. Since the experimental data did not provide a direct measurement of the hydrodynamic impact force as such, the measured hull accelerations were used as a close approximation for the hydrodynamic impact force. Although, as discussed in reference 2, the hull acceleration may not be equal to the hydrodynamic impact acceleration because of elastic effects, for the tested seaplane, in which the rigid hull-support struts were attached to the wing in the immediate vicinity of the fundamental and secondary flexural nodal points, the effect of wing elasticity on the hull accelerations was minimized. Thus, the measured hull accelerations presented in table II and figure 5 can be considered as being a very close approximation to the actual applied landing reaction and so are considered to be the translational component of wing-tip accelerations for the test seaplane. Since the sine curve has been shown to be a good approximation for the measured hull accelerations of the test seaplane this curve is used to define the time history of the translational component of acceleration and also, as shown in the following section, to calculate the transient oscillatory component of acceleration.

Transient oscillatory component of acceleration.- As shown by equation (9), the evaluation of the transient oscillatory component of acceleration for any point on the wing associated with the vibration of any particular wing bending mode has been reduced to the solution of the differential equations of motion of an equivalent single-mass oscillator of frequency equal to the natural frequency of the wing bending mode being considered and of effective spring constant k_e as defined by equations (7) and (8). The time history of the

acceleration $\ddot{y}$ of this single-mass oscillator when subjected to a forcing function of sine-curve variation is derived in the appendix for the case of no damping. Substituting k_e for k in equation (A6) results in the expression

$$\ddot{y} = \frac{P_{max}\omega_n^2}{k_e}\left\{\sin\left(\frac{\pi}{2t_i}\right)t - \left[\frac{1}{\left(\frac{t_n}{t_i}\right)^2 - 1}\right]\left[\frac{t_n}{t_i}\sin\omega_n t - \sin\left(\frac{\pi}{2t_i}\right)t\right]\right\} \quad (10)$$

The use of equation (8) gives the following expression for $\ddot{y}$:

$$\ddot{y}_x = \phi_x \frac{P_{max}\omega_n^2}{k_{e_{tip}}}\left\{\sin\left(\frac{\pi}{2t_i}\right)t - \left[\frac{1}{\left(\frac{t_n}{t_i}\right)^2 - 1}\right]\left[\frac{t_n}{t_i}\sin\omega_n t - \sin\left(\frac{\pi}{2t_i}\right)t\right]\right\} \quad (11)$$

This expression for the transient oscillatory component of acceleration at any point x on the wing corresponds to the term $\phi\ddot{y}_t$ of equation (2). Thus,

$$\ddot{y}_t = \frac{P_{max}\omega_n^2}{k_{e_{tip}}}\left\{\sin\left(\frac{\pi}{2t_i}\right)t - \left[\frac{1}{\left(\frac{t_n}{t_i}\right)^2 - 1}\right]\left[\frac{t_n}{t_i}\sin\omega_n t - \sin\left(\frac{\pi}{2t_i}\right)t\right]\right\} \quad (12)$$

The sine-curve function is used for $P(t)$ because it agrees closely with the measured hydrodynamic-force time history, as shown in figure 5.

In equation (10), P_{max} and t_i are characteristics of the forcing function. Both quantities are given in table II where P_{max} is expressed as acceleration in multiples of the gross weight of the seaplane. The values of the terms ω_n and t_n are also readily known since they are dependent upon the frequency of the wing bending mode being considered. The spring constant k_e is derived from equations (7) and (8). Values of k_e, in the fundamental bending mode of vibration of the wing, are shown in table III for many stations along the wing. In particular, the value of k_e at the wing-tip-accelerometer station is shown to be -336,400 pounds per foot.

An effective spring constant can also be found for the secondary wing bending mode by following a procedure similar to that illustrated in table III, using values of ϕ^2 given in table I. This constant was not calculated in this paper, however, since the strut-support point on the wing coincides almost exactly with the inboard nodal point of the secondary mode. This location results in extremely small deflections of this mode and consequently minimizes the contribution of this mode to the total wing-tip accelerations.

An examination of equation (10) shows that the term $P_{max}\omega_n^2/k_e$ is the acceleration of the effective mass $\left(k_e/\omega_n^2\right)$ for the point on the wing corresponding to k_e if this effective mass is considered to be a springless mass subjected to a force P_{max}. The expression in braces represents the transient-acceleration response to a sine curve of the linear single-mass oscillator expressed in terms of ω_n and in terms of the ratio of natural period to impact period t_n/t_i. Solutions of equation (10) were made for a unit value of $P_{max}\omega_n^2/k_e$, for a value of ω_n equal to the natural frequency of the fundamental mode of the wing of the test seaplane, and for values of the ratio t_n/t_i ranging from 0.1 to 0.7. This range of values of t_n/t_i includes all the landings listed in table II.

Shown in figure 6 are half cycles of the sine-curve time histories of impact forces of various assumed impact periods, expressed in terms of values of t_n/t_i, and also shown are the solutions of equation (10) which are the resulting time histories of the transient-acceleration response referred to thereon as transient-oscillatory acceleration factor. A time scale is included in this figure in order to make the results generally applicable to other values of ω_n. This form of presentation of results illustrates the phase relation between both components of acceleration for different values of t_n/t_i. The sine-curve time histories are representative of the time-history variation of the translational component of the resultant acceleration whereas the time histories in the lower plot define the transient-oscillatory component of resultant acceleration. Application of these graphical results to the calculation of the resultant acceleration at the wing-tip-accelerometer station is discussed in the following section on resultant wing-tip accelerations.

The evaluation of the acceleration response factor was not carried beyond time $2t_i$ since, if the equations as set up in the appendix were

extended to times longer than $2t_i$, the results would not correspond to a sine pulse but, rather, to a continuous application of the sine-curve forcing function. For values of t_n/t_i equal to or less than approximately 0.7 the maximum oscillatory acceleration occurs prior to $2t_i$ so that the plots in figure 6 are applicable to all runs of the tested seaplane. Further, for most present-day seaplanes, the maximum design impact loads are usually applied at such a rate that the ratio t_n/t_i rarely exceeds values of 0.7. In cases where the value of the ratio t_n/t_i is such that the maximum oscillatory component occurs at times later than $2t_i$, the response curves in figure 6 may be extended to cover the case of a sine pulse by considering the single-mass oscillator to start vibrating freely from initial condition of displacement and velocity corresponding to time $2t_i$. In any case, if the maximum oscillatory acceleration occurs at times substantially later than the occurrence of maximum impact load, a check on the agreement between the assumed sine curve and the measured-hydrodynamic-force since curve should be made since, as shown in this paper, the assumed and actual time histories were in disagreement at times substantially later than t_i.

Resultant wing-tip acceleration.- For the tested seaplane, addition of the time histories of the translational component of acceleration, equation (3), and transient oscillatory component of acceleration associated with the vibration in the fundamental wing bending mode, equation (11), gives the resultant time history of acceleration for any point x on the wing. This is expressed by the following equation:

$$\ddot{y}_r = \frac{P_{max} \sin \omega_i t}{M} + \phi_x \frac{P_{max}\, \omega_n^2}{k_{e_{tip}}} \left\{ \sin \omega_i t - \left[\frac{1}{\left(\frac{t_n}{t_i}\right)^2 - 1} \right] \left[\frac{t_n}{t_i} \sin \omega_n t - \sin \omega_i t \right] \right\} \tag{13}$$

The acceleration computed from equation (13) is in units of displacement per second^2. In order to compute the acceleration in multiples of the acceleration due to gravity, as was done throughout this paper, each

term of equation (13) must be divided by the quantity g. Equation (13) then becomes

$$\frac{\ddot{y}_r}{g} = \frac{P_{max}}{W} \sin \omega_i t + \phi_x \frac{P_{max}\omega_n^2}{gk_{e_{tip}}} \left\{ \sin \omega_i t - \left[\frac{1}{\left(\frac{t_n}{t_i}\right)^2 - 1} \right] \left[\frac{t_n}{t_i} \sin \omega_n t - \sin \omega_i t \right] \right\} \tag{14}$$

where W is the total weight of the airplane.

The force applied to the wing at the strut-support point P_{max} is most conveniently expressed in multiples of airplane weight. That is,

$$P_{max} = n_i W \tag{15}$$

where n_i = maximum impact acceleration in multiples of the acceleration due to gravity. Equation (14) then becomes

$$\frac{\ddot{y}_r}{g} = n_i \sin \omega_i t + \phi_x n_i \frac{W\omega_n^2}{gk_{e_{tip}}} \left\{ \sin \omega_i t - \left[\frac{1}{\left(\frac{t_n}{t_i}\right)^2 - 1} \right] \left[\frac{t_n}{t_i} \sin \omega_n t - \sin \omega_i t \right] \right\} \tag{16}$$

which is the equation evaluated by the tabulations given in table IV and table V.

The calculations concerned with the evaluation of the resultant-wing-tip-acceleration time histories are given in table IV. The translational and oscillatory acceleration factors used in these calculations were interpolated from figure 6. The value of t in seconds is directly equal to the value of C_t in figure 6, since, for the fundamental frequency, the value of $0.0525/t_n$ is unity. The values of translational

acceleration were obtained by multiplying the maximum impact acceleration by the translational acceleration factor. The values of oscillatory acceleration were obtained by multiplying the maximum impact acceleration by the oscillatory acceleration factor and by the factor −1.56 which is the term $\phi_x \frac{W\omega_n^2}{gk_{e_{tip}}}$ in equation (16). The value of W in this term is 19,200 pounds, ω_n is equal to $4.67(2\pi)$ radians per second, and $k_{e_{tip}}$ is the effective spring constant for the actual wing tip in the fundamental wing bending mode, shown in table III to be equal to −252,300 pounds per foot.

As an alternative for carrying out a time-history solution like those for runs 2, 3, and 7, the peak acceleration can be approximated by carrying out the calculation for resultant acceleration by use of the values of the acceleration factors corresponding to the time of maximum negative transient-oscillatory-acceleration factor as shown in figure 6. Maximum wing-tip accelerations for all test runs calculated by this method are presented in table V. As a check on the adequacy of this approximate method, it will be seen that the maximum accelerations for runs 2, 3, and 7, as obtained by the time-history solution (table IV), agree closely with the maximum values of acceleration listed in table V.

It is interesting to note from figure 6 that as the ratio t_n/t_i attains large values the maximum transient-oscillatory-acceleration factor occurs at reduced values of the translational acceleration described by the sine curve. Methods of determining maximum accelerations that suggest the addition of peak acceleration values in each mode without regard to phase may thus lead to resultant accelerations that are unduly conservative for these large values of t_n/t_i. The peak oscillatory components of acceleration for small values of t_n/t_i occur at very nearly the time of maximum translational acceleration.

Comparison of Experimental and Calculated Results

A comparison between the calculated wing-tip-acceleration time histories given in table IV and the experimentally obtained wing-tip accelerations is presented in figure 5. The agreement between theory and experiment is good insofar as the negative values of the acceleration are concerned but a slight discrepancy is noticed in the positive values during the initial stages of the impact. The exact cause of this discrepancy is unknown, but it may be due to the fact that the true hydrodynamic forcing function is actually applied at a slower rate at the time of impact than that represented by the assumed sine-curve variation. The time-history solutions of tip acceleration were not extended very much beyond the time of maximum acceleration since the assumed sine curve deviates appreciably from the measured forcing function in this range. This general agreement between the experimental acceleration and the theoretical acceleration calculated by considering only the effect of the fundamental bending mode substantiates the assumption that, for the

tested seaplane, the effects of the secondary and higher bending modes on the resultant acceleration were small.

Figure 7 presents a comparison between the computed maximum negative wing-tip accelerations given in table V and the corresponding experimental maximum wing-tip accelerations given in table II. Although there is some scatter of test points, the agreement between theory and experiment is satisfactory.

It should be remembered that the agreement obtained between the theoretical and experimental acceleration time histories and the peak values of wing-tip acceleration are, in the case of the tested seaplane, for an airframe wherein only the primary bending mode was important and wherein the structural elasticity has a small effect on the hydrodynamic load. Although the method used may be extended to include an evaluation of the combined effects of several bending modes, the small contribution of the higher bending modes of the test seaplane to total wing-tip acceleration precluded the inclusion of these higher modes.

CONCLUSIONS

Experimental wing-tip-acceleration data obtained from full-scale landing tests of a small seaplane were compared with the analytical wing-tip accelerations calculated by application of a simplified method of analysis. The structural characteristics of the seaplane were such that only the fundamental wing bending mode had an important effect on the wing-tip acceleration and the over-all structural properties had a small effect on altering the hydrodynamic load. The results of the comparison indicate that, for the tested seaplane and for the conditions of impact encountered, the following conclusions may be drawn:

1. The method of calculating the acceleration response at any wing station by using an equivalent single-mass linear oscillator to represent the vibratory properties of that station gave good agreement between the measured and calculated time histories of wing-tip acceleration.

2. For the impacts encountered, the assumed sine-curve variation of hydrodynamic impact force showed good agreement with the experimentally determined variation up to and somewhat beyond the time of maximum impact load.

3. With large ratios of natural vibratory period to impact period the maximum transient-oscillatory-acceleration component occurs subsequent to the time of maximum translational acceleration so that phase relations should be used in computing the distribution of maximum accelerations in the wing.

4. When the most severe impacts of the tested seaplane occurred subsequent to the initial impact of a particular landing, the seaplane bounce that preceded this severe impact was usually sufficiently high and of long enough duration to stop the wing vibration excited by the prior impact.

Langley Aeronautical Laboratory
National Advisory Committee for Aeronautics
Langley Field, Va., April 2, 1948

APPENDIX

EQUATION OF TRANSIENT ACCELERATION OF A SINGLE-MASS LINEAR OSCILLATOR WHEN SUBJECTED TO A SINE-CURVE FORCING FUNCTION

An elastic, single-mass system having only one degree of freedom and no damping can be schematically represented by the following sketch:

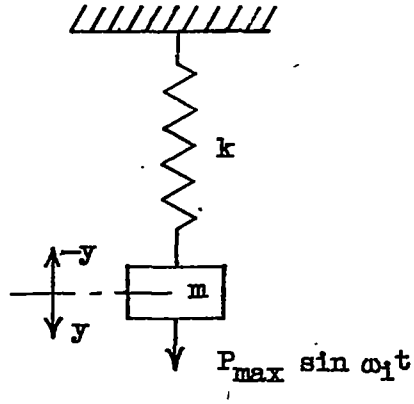

The dynamics of this system when subjected to a force of sine-curve time-history variation can be expressed as the following differential equation:

$$m\ddot{y} + ky = P_{max} \sin \omega_1 t \qquad (A1)$$

where

y	displacement due to applied force
m	mass of system
k	spring constant
P_{max}	maximum value of applied force

ω_i equivalent circular frequency of applied force, radians per second $(\pi/2t_i)$

t time elapsed after initial water contact, seconds

t_i time between initial water contact and maximum hydrodynamic force, seconds

The time history of the displacement of a single-mass system, as shown in the sketch, due to any arbitrary forcing function $F(\tau)$ can be evaluated by the integral

$$y = \frac{1}{\omega_n m} \int_0^t F(\tau) \sin\left[\omega_n(t - \tau)\right] d\tau \tag{A2}$$

where τ is the variable of integration. This integral will be reorganized to be the Duhamel integral, the derivation of which is given in reference 4. Replacing the arbitrary forcing function $F(\tau)$ in the Duhamel integral by the sine-curve variation of the forcing function $P_{max} \sin \omega_i \tau$ and substituting this value of displacement in equation (A1) gives the solution for acceleration $\ddot{y}$ of the mass as

$$\ddot{y} = \frac{P_{max} \sin \omega_i t}{m} - \frac{\omega_n}{m} \int_0^t P_{max} \sin\left[\omega_i \tau(t - \tau)\right] d\tau \tag{A3}$$

Carrying through the integration of equation (A3) results in

$$\ddot{y} = \frac{P_{max} \sin \omega_i t}{m} - \frac{P_{max}}{m}\left[\frac{1}{\left(\frac{\omega_i}{\omega_n}\right)^2 - 1}\right]\left(\frac{\omega_i}{\omega_n} \sin \omega_n t - \sin \omega_i t\right) \tag{A4}$$

Expressing $\ddot{y}$ in terms of t_n and t_i and replacing ω_i by $(\pi/2t_i)$ and m by k/ω_n^2 gives

$$\ddot{y} = \frac{P_{max}\,\omega_n^2 \sin\left(\frac{\pi}{2t_i}\right)t}{k} - \frac{P_{max}\,\omega_n^2}{k}\left[\frac{1}{\left(\frac{t_n}{t_i}\right)^2 - 1}\right]\left[\frac{t_n}{t_i}\sin \omega_n t - \sin\left(\frac{\pi}{2t_i}\right)t\right] \tag{A5}$$

Simplifying equation (A5) reduces the expression for $\ddot{y}$ to

$$\ddot{y} = \frac{P_{max}\,\omega_n^2}{k}\left\{\sin\left(\frac{\pi}{2t_i}\right)t - \left[\frac{1}{\left(\frac{t_n}{t_i}\right)^2 - 1}\right]\left[\frac{t_n}{t_i}\sin \omega_n t - \sin\left(\frac{\pi}{2t_i}\right)t\right]\right\} \tag{A6}$$

The acceleration expressed by equation (A6) is used to define the oscillatory components of the total acceleration at any point in the wing structure when the natural-vibration characteristics of that wing station are replaced by an equivalent single-mass oscillator as described in the body of the paper. It will be seen from this equation that when the ratio t_n/t_i approaches zero (corresponding to an extremely slow rate of application of the impulsive load) the acceleration $\ddot{y}$ defined by equation (A6) approaches zero. This fact indicates that the oscillatory effects are negligible. For airplanes subjected to such a very slowly applied load, the acceleration of all points on the structure is nearly the same and nearly equal to the translational acceleration. Equation (A6) is plotted in the lower set of curves of figure 6 of this paper for values of t_n/t_i ranging from 0.1 to 0.7 and for $\frac{P_{max}\,\omega_n^2}{k} = 1$, and is identified thereon as the "transient-oscillatory acceleration factor." A time-scale correction factor is included in figure 6 to make the results generally applicable for all values of ω_n.

REFERENCES

1. Biot, M. A., and Bisplinghoff, R. L.: Dynamic Loads on Airplane Structures during Landing. NACA ARR No. 4H10, 1944.

2. Mayo, Wilbur L.: Solutions for Hydrodynamic Impact Force and Response of a Two-Mass System with an Application to an Elastic Airframe. NACA TN No. 1398, 1947.

3. Mayo, Wilbur L.: Analysis and Modification of Theory for Impact of Seaplanes on Water. NACA Rep. No. 810, 1945.

4. Von Kármán, Theodore, and Biot, Maurice A.: Mathematical Methods in Engineering. First ed., McGraw-Hill Book Co., Inc., 1940.

TABLE I

WEIGHT DISTRIBUTION AND MODE-SHAPE FACTORS OF WING SEMISPAN

Distance from center line (in.)	Increment of weight, w (lb)	Mode-shape factor	
		First mode (4.76 cps), ϕ	Second mode (13.00 cps), ϕ'
0	----	-0.045	-0.061
31	881	-.044	-.047
75	2057	-.026	-.017
87.7	5076	-.022	-.005
119	881	-.004	.037
170	116	.053	.122
210	102	.110	.194
250	88	.190	.238
290	181	.270	.242
330	64	.370	.184
370	53	.490	.041
410	43	.625	-.177
440	18	.730	-.388
477.7	40	.860	-.681
516	----	1.000	-1.000
Total	9600		

NACA

TABLE II

EXPERIMENTAL MAXIMUM ACCELERATIONS DURING LANDING IMPACT

Test run	Impact	Max. hull acceleration (g)	Time to max. hull acceleration, t_i (sec)	Max. wing-tip acceleration (g)
1	third	−1.15	0.270	−1.75
2	second	−1.52	.150	−2.75
3	second	−1.90	.085	−4.25
4	second	−.92	.270	−1.30
5	third	−.90	.143	−1.45
6	fourth	−.84	.120	−1.75
7	first	−1.85	.190	−2.60
8	second	−1.25	.195	−2.35
9	second	−.95	.300	−1.52
10	second	−1.00	.120	−1.68
11	third	−.92	.150	−1.40
12	fourth	−.85	.125	−1.45
13	second	−.95	.130	−1.40
14	third	−.60	.290	−.70
15	first	−.85	.120	−1.68

TABLE III

EFFECTIVE SPRING CONSTANTS ALONG WING SEMISPAN IN FUNDAMENTAL MODE

Distance from center line, x (in.)	Increment of weight, w (lb)	Mode-shape factor[a], ϕ	Increment of effective weight, $W\phi^2$	Effective spring constant, k_e (lb/ft)
0	----	-0.045	------	5,606,670
31	881	-.044	1.707	5,734,090
75	2057	-.026	1.391	9,703,850
87.7	5076	-.022	2.460	11,468,180
119	881	-.004	.014	63,075,000
170	116	.053	.329	-4,760,040
210	102	.110	1.232	-2,293,640
250	88	.190	3.173	-1,327,890
290	181	.270	13.230	-934,440
330	64	.370	8.769	-681,890
370	53	.490	12.789	-514,890
410	43	.625	16.813	-403,680
440	18	.730	9.563	-345,620
477.7	40	.860	29.584	-293,370
516	----	1.000	------	-252,300
Total	9600		101.054	

[a]For unit tip deflection with respect to nodal point, see figure 4.

Sample calculations for effective spring constant

(a) For wing tip

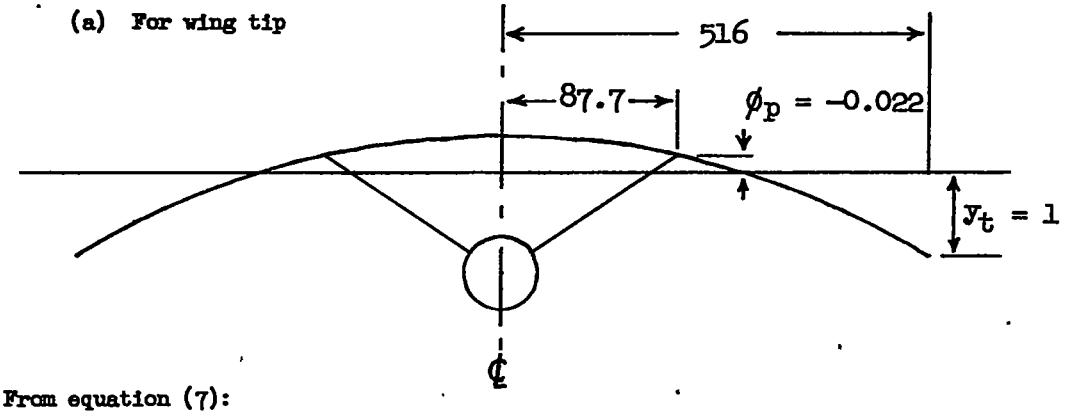

From equation (7):

$$k_{e_{tip}} = \frac{\omega_n^2 \Sigma m\phi^2}{\phi_p} = \frac{(4.76 \times 2\pi)^2}{-0.022} \frac{(2 \times 101.054)}{32.2} = -252{,}300 \text{ lb/ft}$$

(b) For point of location of wing-tip accelerometer

Effective spring constant at 450 inches from center line is obtained by application of equation (8); thus:

$$k_{e_{450}} = \frac{k_{e_{tip}}}{\phi_{450}} = \frac{-252300}{0.75} = -336{,}400 \text{ lb/ft}$$

TABLE IV

CALCULATED TIME HISTORIES OF RESULTANT WING-TIP (STATION 450) ACCELERATIONS FOR SEVERE IMPACTS

[Only the effect of the fundamental bending mode of vibration (t_n = 0.0325 sec) is included]

Time after contact, t (sec)	Test run 2 n_i = -1.52g; t_i = 0.150 sec; $\frac{t_n}{t_i}$ = 0.35					Test run 3 n_i = -1.90g; t_i = 0.085 sec; $\frac{t_n}{t_i}$ = 0.61					Test run 7 n_i = -1.85g; t_i = 0.190 sec; $\frac{t_n}{t_i}$ = 0.28				
	Translational acceleration factor[a]	Oscillatory acceleration factor[a]	Translational acceleration[b]	Oscillatory acceleration[c]	Resultant acceleration[d]	Translational acceleration factor[a]	Oscillatory acceleration factor[a]	Translational acceleration[b]	Oscillatory acceleration[c]	Resultant acceleration[d]	Translational acceleration factor[a]	Oscillatory acceleration factor[a]	Translational acceleration[b]	Oscillatory acceleration[c]	Resultant acceleration[d]
0.01	0.10	0.10	-0.15	0.24	0.09	0.18	0.18	-0.34	0.54	0.20	0.08	0.08	-0.15	0.24	0.09
.02	.20	.19	-.30	.46	.16	.36	.34	-.65	1.03	.38	.17	.16	-.31	.47	.16
.03	.30	.24	-.46	.58	.12	.52	.45	-.99	1.35	.36	.24	.21	-.44	.62	.18
.04	.40	.31	-.61	.73	.14	.67	.51	-1.27	1.54	.27	.31	.25	-.57	.74	.17
.05	.49	.33	-.74	.80	.06	.79	.50	-1.50	1.51	.01	.38	.26	-.70	.76	.06
.06	.57	.30	-.87	.73	-.14	.89	.42	-1.69	1.27	-.42	.46	.23	-.85	.74	-.11
.07	.66	.24	-1.00	.58	-.42	.95	.29	-1.81	.88	-.93	.54	.21	-1.00	.62	-.38
.08	.72	.16	-1.09	.39	-.70	.99	.05	-1.88	.15	-1.73	.61	.14	-1.13	.41	-.72
.09	.79	.09	-1.20	.12	-1.08	.99	-.18	-1.88	-.34	-2.22	.67	.04	-1.24	.12	-1.12
.10	.85	-.07	-1.29	-.17	-1.46	.96	-.44	-1.82	-1.33	-3.15	.73	-.02	-1.35	-.06	-1.41
.11	.90	-.20	-1.37	-.48	-1.85	.89	-.68	-1.69	-2.05	-3.74	.78	-.11	-1.44	-.32	-1.76
.12	.92	-.32	-1.40	-.77	-2.17	.80	-.92	-1.52	-2.78	-4.30	.83	-.21	-1.54	-.62	-2.16
.13	.96	-.42	-1.46	-1.02	-2.48	.66	-1.08	-1.25	-3.26	-4.51	.88	-.28	-1.63	-.82	-2.45
.14	.97	-.49	-1.47	-1.18	-2.65	.54	-1.17	-1.03	-3.53	-4.56	.91	-.34	-1.68	-1.00	-2.68
.15	.98	-.54	-1.49	-1.31	-2.80	.36	-1.16	-.68	-3.50	-4.18	.94	-.38	-1.74	-1.12	-2.86
.16	.99	-.55	-1.50	-1.33	-2.88						.96	-.38	-1.78	-1.12	-2.90
.17	.98	-.52	-1.49	-1.26	-2.75						.97	-.37	-1.79	-1.08	-2.87
.18	.94	-.44	-1.43	-1.06	-2.49						.98	-.33	-1.81	-.97	-2.78
.19	.90	-.35	-1.37	-.85	-2.22						.98	-.25	-1.81	-.74	-2.55
.20	.84	-.23	-1.28	-.56	-1.84						.99	-.16	-1.83	-.47	-2.30

[a]Translational and oscillatory acceleration factors interpolated from figure 6.

[b]Translational acceleration = (Translational acceleration factor) (Maximum impact acceleration).

[c]Oscillatory acceleration = (Oscillatory acceleration factor) (Maximum impact acceleration) (-1.59).

[d]Resultant acceleration = Translational acceleration + Oscillatory acceleration.

TABLE V

CALCULATED MAXIMUM WING-TIP ACCELERATIONS FOR ALL TEST RUNS

[Only the effect of the fundamental mode of vibration (t_n = 0.0525 sec) is included]

Test run	Maximum hull acceleration, n_i (g)	t_n/t_i	Maximum oscillatory acceleration factor	Translational acceleration factor[a]	Maximum oscillatory acceleration[b] (g)	Translational acceleration[c] (g)	Resultant acceleration (g)
1	-1.15	0.19	-0.24	0.79	-0.44	-0.91	-1.35
2	-1.52	.35	-.54	.96	-1.31	-1.46	-2.77
3	-1.90	.61	-1.14	.56	-3.44	-1.06	-4.50
4	-.92	.19	-.24	.79	-.35	-.73	-1.08
5	-.90	.37	-.57	.96	-.81	-.86	-1.67
6	-.84	.44	-.76	.90	-1.02	-.76	-1.78
7	-1.85	.28	-.38	.94	-1.12	-1.74	-2.86
8	-1.25	.27	-.37	.95	-.74	-1.19	-1.93
9	-.95	.18	-.21	.88	-.32	-.84	-1.16
10	-1.00	.44	-.76	.90	-1.20	-.90	-2.10
11	-.92	.35	-.54	.96	-.79	-.88	-1.67
12	-.85	.42	-.73	.92	-.99	-.78	-1.77
13	-.95	.40	-.66	.94	-1.00	-.89	-1.89
14	-.60	.18	-.21	.75	-.20	-.45	-.65
15	-.85	.44	-.76	.90	-1.03	-.77	-1.80

[a]Taken at time of maximum oscillatory acceleration factor in figure 6.

[b]Maximum oscillatory acceleration = (Maximum oscillatory acceleration factor) (Maximum hull acceleration) (-1.59).

[c]Translational acceleration = (Translational acceleration factor) (Maximum hull acceleration).

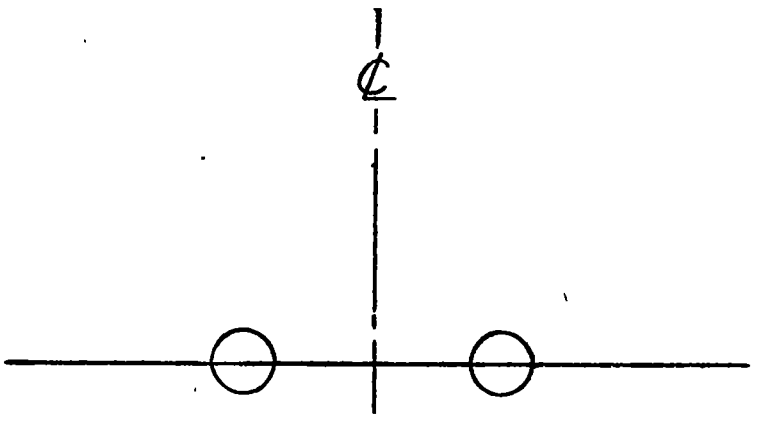

(a) Simplified representation of airplane wing and fuselage.

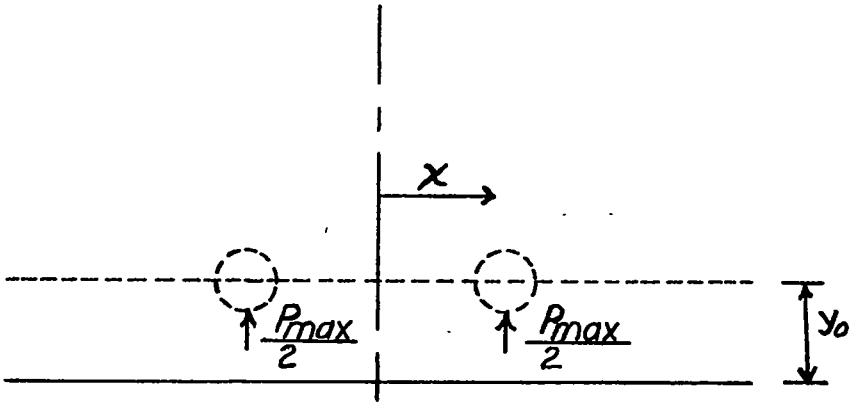

(b) Translational motion of airplane wing and fuselage as rigid body.

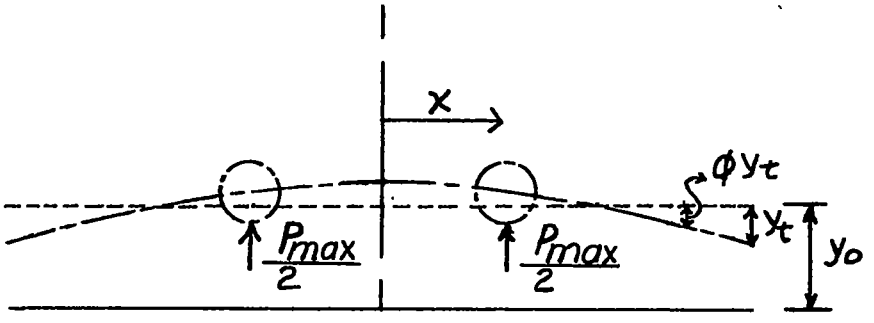

(c) Oscillatory motion of natural mode of wing and fuselage combination superposed on translational motion of airplane.

Figure 1.- Simplified representation of translational and oscillatory components of motion of points along wing.

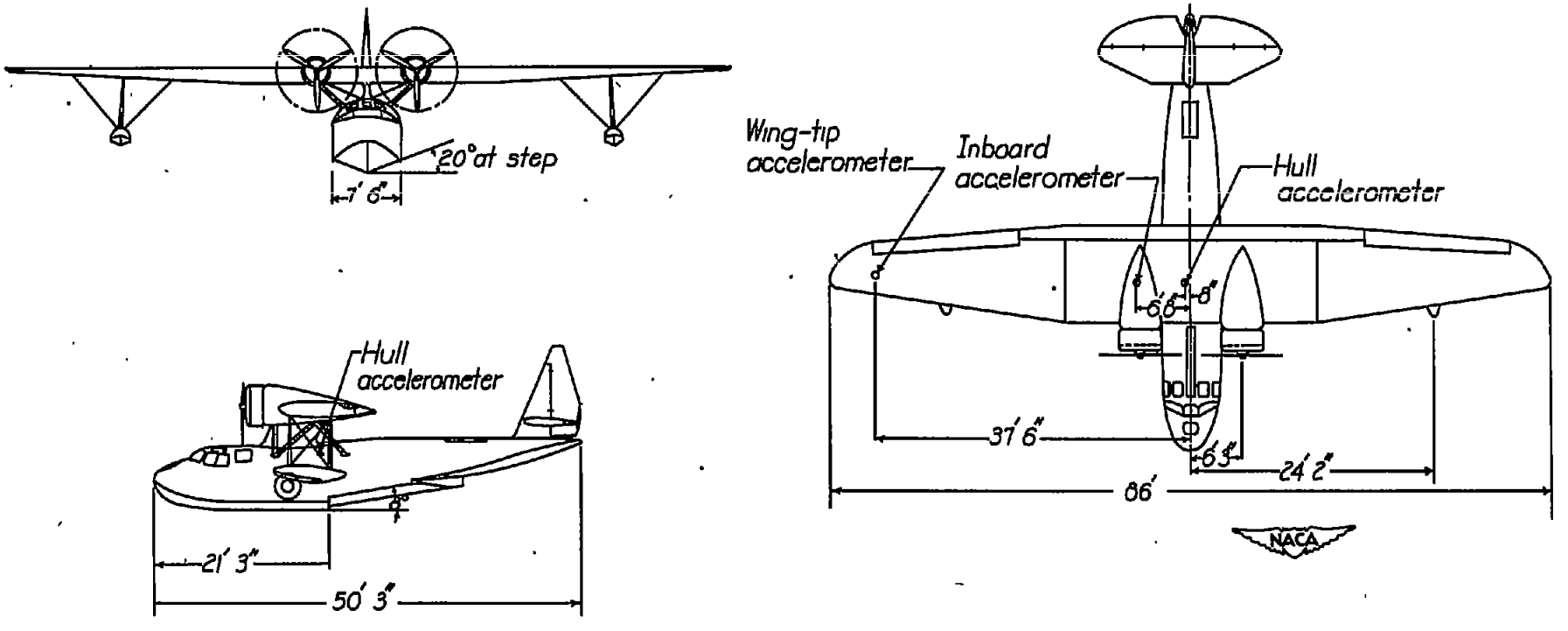

Figure 2.- General arrangement of seaplane and accelerometers.

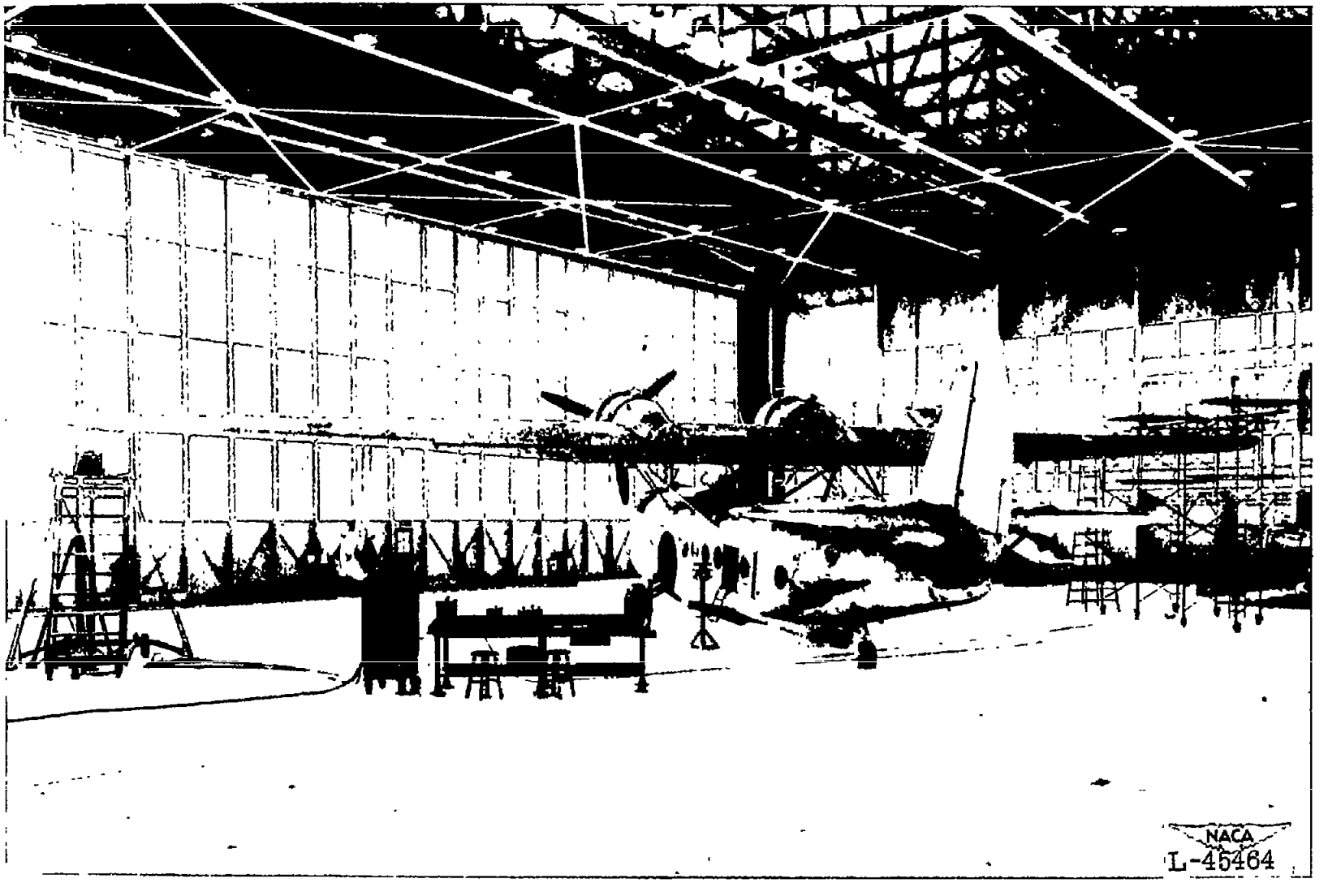

Figure 3.- Setup of seaplane during ground vibration tests.

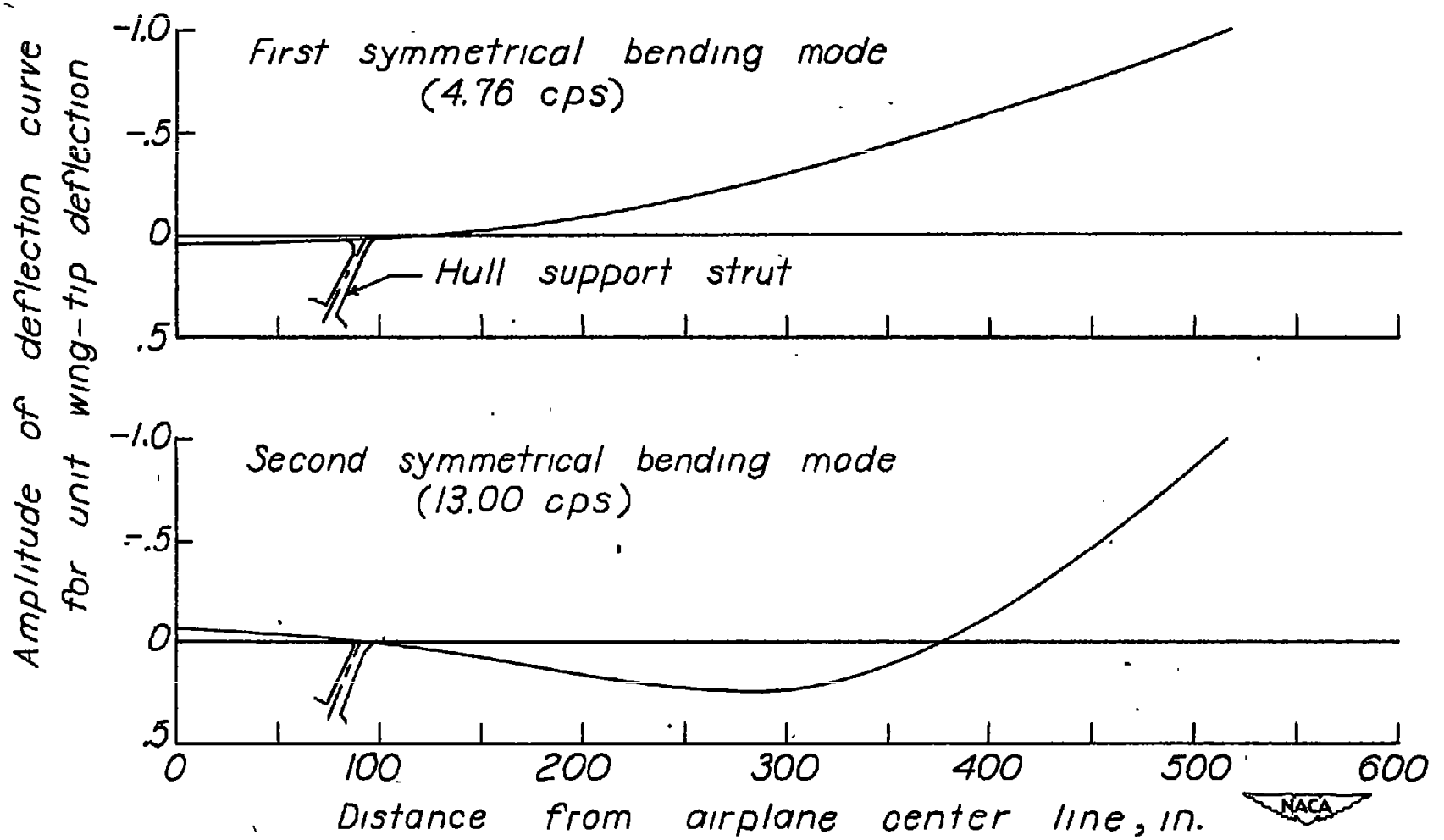

Figure 4.- Symmetrical bending-mode shapes of wing semispan.

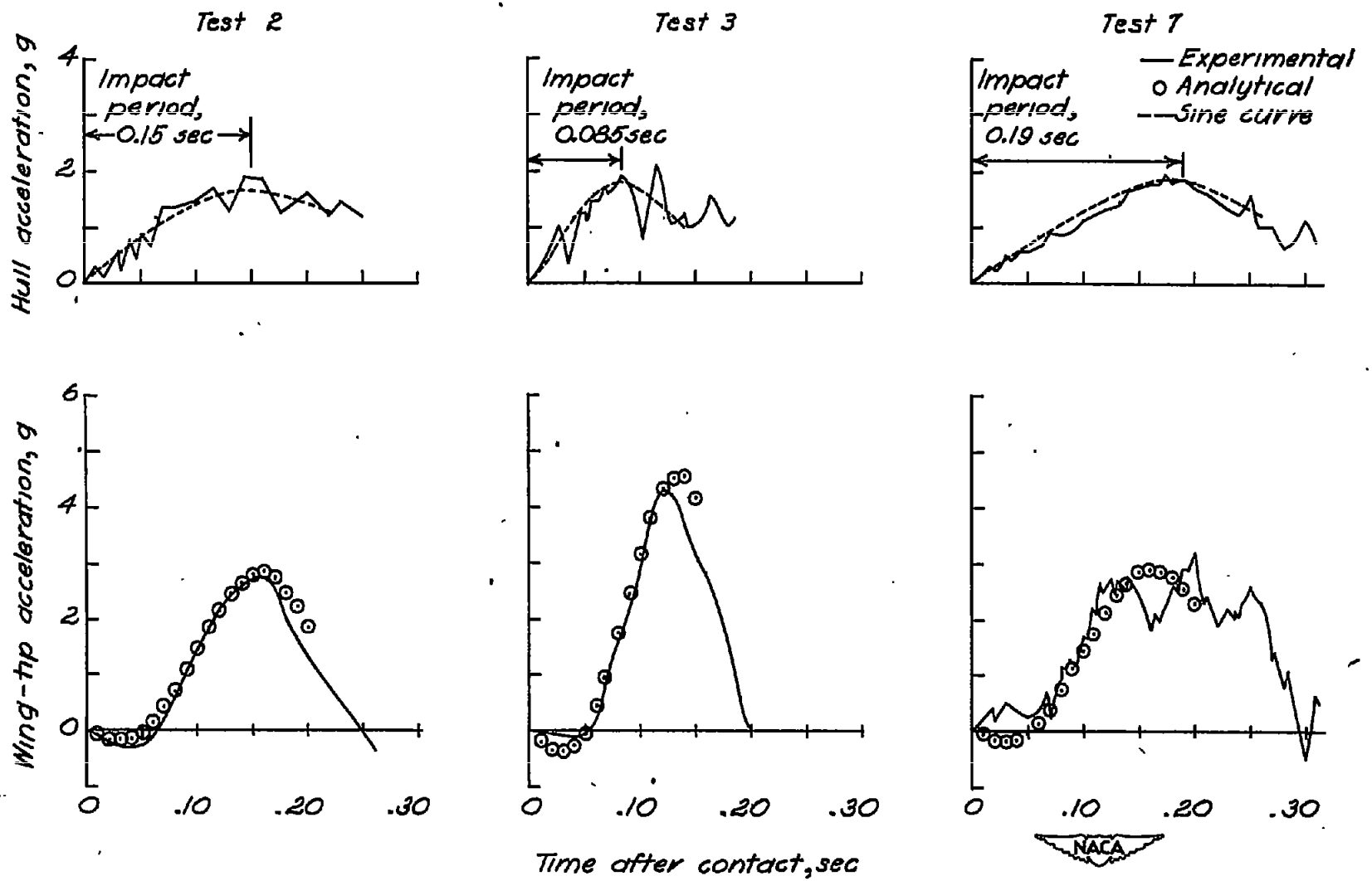

Figure 5.- Time histories of hull and wing-tip accelerations for test runs 2, 3, and 7.

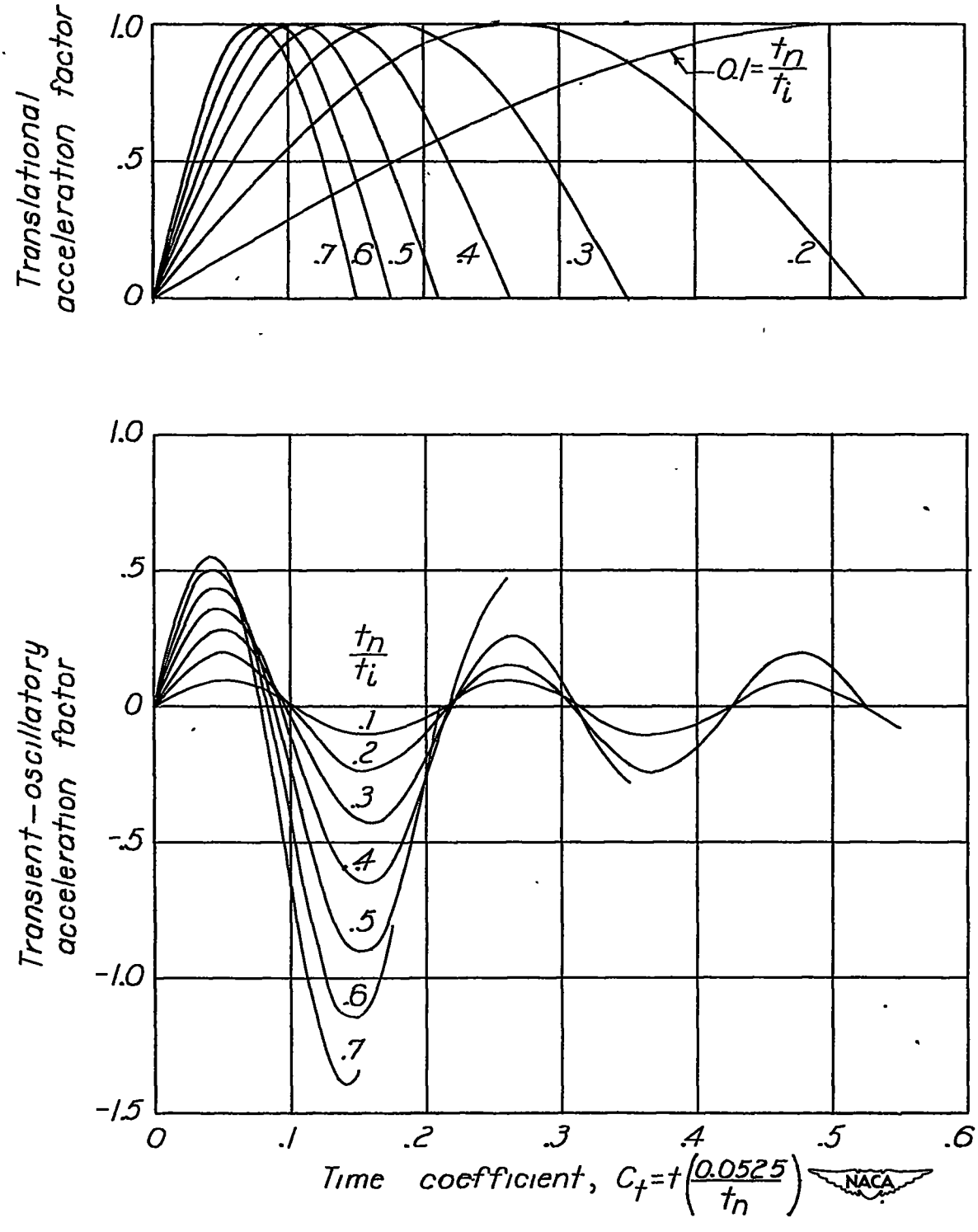

Figure 6.- Time histories of acceleration factors for sine-curve forcing function of unit load and various values of $\frac{t_n}{t_i}$.

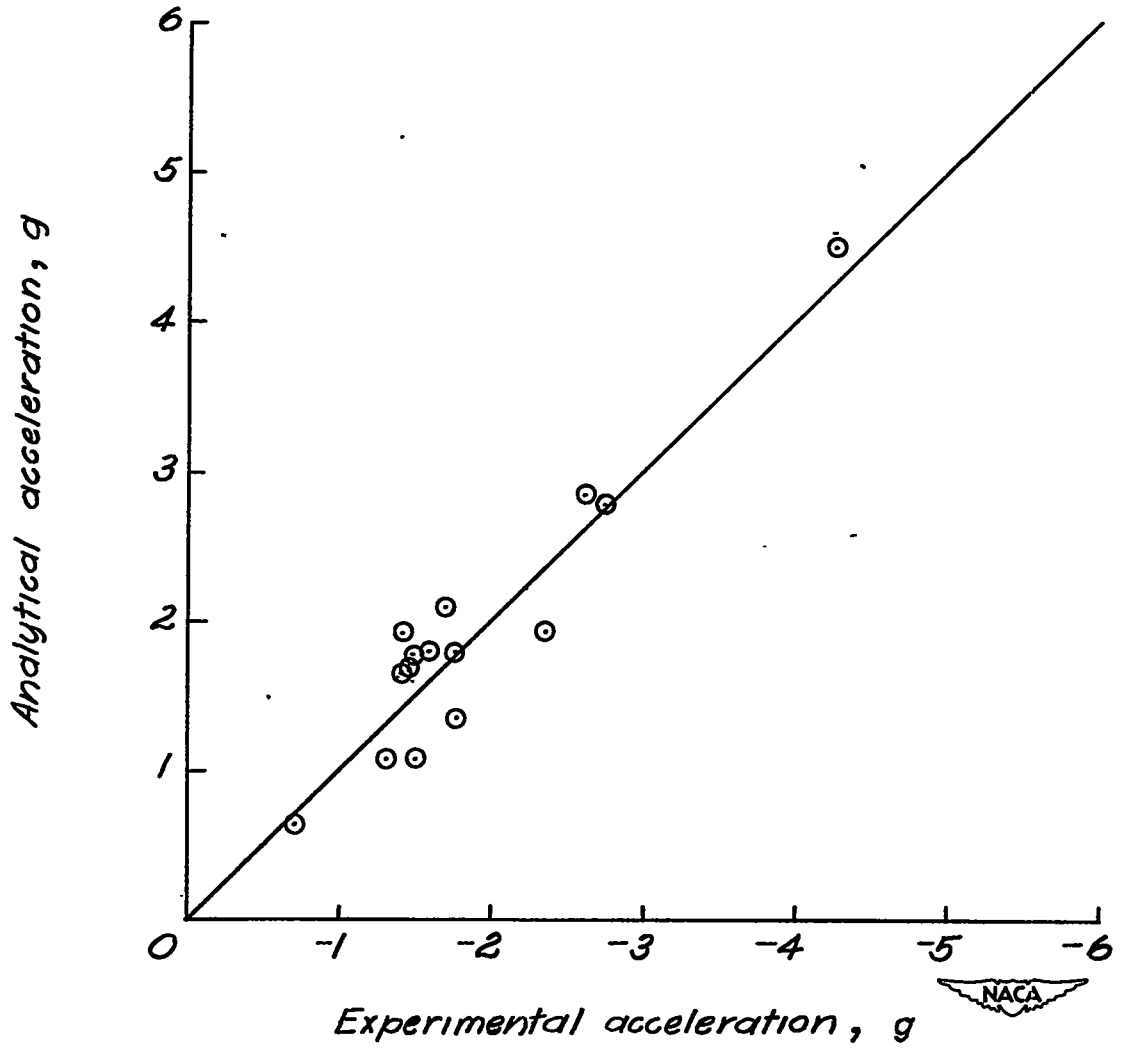

Figure 7.- Comparison of maximum experimental and analytical wing-tip accelerations.